Received: 26 October 2023 | Accepted: 1 March 2024

DOI: 10.1111/arcm.12971

ORIGINAL ARTICLE

Historical lime-based flooring mortars from the Church of Santa Maria de Alcobaça monastery (12th century), Portugal: A multi-analytical approach

Fernanda Carvalho[1,2] | **Ana Nunes**[3] | **Ana Pagará**[4] | **Isabel Costeira**[4] | **Teresa Pereira da Silva**[5] | **Maria Margarida Rolim Augusto Lima**[1,2] | **João Pedro Veiga**[1,6]

[1]CENIMAT/i3N—Centro de Investigação de Materiais, Caparica, Portugal

[2]Department of Materials Science, Caparica, Portugal

[3]Direção Geral do Património Cultural—DGPC, Lisbon, Portugal

[4]Mosteiro de Alcobaça, Alcobaça, Portugal

[5]LNEG—Laboratório Nacional de Energia e Geologia, I.P., Unidade de Recursos Minerais e Geofísica, Amadora, Portugal

[6]Department of Conservation and Restoration, Caparica, Portugal

Correspondence
F.Carvalho and J.P. Veiga, CENIMAT/i3N—Centro de Investigação de Materiais, FCT NOVA, 2829-516 Caparica, Portugal.
Email: fb.carvalho@campus.fct.unl.pt and jpv@fct.unl.pt

Funding information
This work was supported by the FEDER funds through the COMPETE 2020 Programme and National Funds through FCT—Portuguese Foundation for Science and Technology under the project ref. UIDB/50025/2020-2023 and SFRH/BD/145308/2019 (F. Carvalho)

Abstract

The Monastery of Alcobaça houses in reserve the ceramic tiles that adorned the floor of the church's apse. These tiles were removed during rehabilitation works and many preserve part of their original fixing mortars. A comprehensive analysis of 21 samples was conducted using a multi-analytical approach (X-ray fluorescence, X-ray diffraction, scanning electron microscopy–energy-dispersive X-ray spectroscopy, μ-Raman spectroscopy, thermogravimetry–differential thermal analysis, optical microscopy, and colorimetry). Results suggest compositional variations in the samples from the back and sides of the ceramic tiles; however, the mineralogy and general characteristics of the aggregates remained consistent between the samples and are coherent with the local geology, suggesting a shared historical origin.

KEYWORDS

built heritage, Cistercian order, flooring, historic mortars

INTRODUCTION

The church of the Monastery of Santa Maria de Alcobaça is one of the most important historical buildings in Portugal. The monastery has been recognized by UNESCO as a World Heritage Site since 1989; it traces its origins to the 12th century and is deeply intertwined with the reconquest of Portuguese territory by King Afonso Henriques. In 1153, the Portuguese king granted a vast expanse of land to the Cistercian Order, which included the region of Alcobaça, for the construction of a monastery. In this way, he would facilitate the region's settlement and elevate at the same time the king's prestige within the Church, solidifying is dominion over the reclaimed territories (Antunes, 2013; de Villamariz, 2012; Ferreira, 1987; Martins, 2011).

The Cistercian Order, founded at the end of the 11th century, embraced a humble monastic life, detached from urban centers, in order to provide a balance between physical toil and spiritual devotion, focused on acts of charity and prayer (Antunes, 2013; de Villamariz, 2012; Ferreira, 1987; Martins, 2015). The value placed on simplicity in all aspects of monastic life was to be reflected even in monastery buildings. This commitment to humility permeated to architectural Cistercian designs, which, though austere, emanated a captivating grandeur through their monumental proportions. Central to this architectural design philosophy was the unifying concept of a Latin cross plan, featuring a central nave flanked by two side naves, culminating in a straight apse. Variations such as apses with radiating chapels and ambulatories also found their place in Cistercian architecture. The blueprint for this design can be traced back to the Abbey of Clairvaux in France, serving as the inspirational template for the construction of the Monastery of Santa Maria de Alcobaça (Antunes, 2013; de Villamariz, 2012).

The chosen location for the monastery in Portugal held rich material resources for construction, with proximity to a limestone massif providing raw materials for stonework and lime production. Oak forests, fertile soils, and nearby river courses, including the Alcoa and Baça rivers, further supported the endeavor (Antunes, 2013). Construction of the church itself began in 1178, 25 years after the monastery was founded, and its consecration dates from 1252. Remarkably, it stands as Portugal's first Gothic construction. The interior's austere ornamentation possibly contrasted with the colorful ceramic flooring that once covered the area at the head of the church. To this day, traces of the original ceramic floor, characterized by its simple shapes and absence of glaze, can be observed in the ambulatory. Subsequent excavation work has revealed a diverse array of shapes and colors, allowing for the assembly of intricate patterns (Colaço, 1932; Simões, 1990). The color palette of this ceramic floor predominantly featured brown, white, turquoise, and green hues, with variations ranging from lighter, opaque tones to deeper, yellowish greens (Carvalho et al., 2016; Trindade, 2007). Recent studies indicate that this pavement would be original, dating back to the 13th century, as evidenced by its formal and chemical characteristics, both in terms of the ceramic body and the color palette and chemical characteristics of the glazes (Carvalho et al., 2016; Trindade, 1998, 2007, 2018).

In the 1930s and 1940s, the then General Directorate of National Buildings and Monuments (DGEMN) undertook heritage restoration and preservation initiatives aimed at restoring the grandeur of national monuments (de Matos, 2019). This project included the removal of all the Baroque decoration of the altar and the radiating chapels added to the church's interior during the 17th and 18th centuries (Antunes, 2013). Beneath the stone slab early ceramic flooring was discovered, but it was initially believed to be Baroque in origin and subsequently removed (de Matos, 2019). The removed pieces were buried in other areas of the monastery and recovered in the late 1990s, after excavation work carried out by the then Portuguese Institute for Architectural and Archaeological Heritage. These preserved fragments, still bearing traces of the mortar that once secured them on their back and/or sides, are now held in reserve.

The design of medieval ceramic tiles used for flooring reflected practical considerations regarding their installation. These tiles typically featured a thick ceramic body more than 2 cm

in thickness, with chamfered edges, allowing space for mortar to spread beneath the tiles and rise along the sides at junction areas, all without overflowing onto the surface. This design facilitated the levelling and fitting of the tiles during the laying process (Durbin, 2005).

Ceramic tiles applied in churches became more popular from the mid-13th century onwards and were commonly laid with lime mortars. Floors could be initially leveled with coarser gravels or stones, followed by the application of a first mortar layer, containing coarser aggregates. The actual laying of the floor would take place in a second stage, involving a thinner mortar layer, allowing for the vertical filling of junction areas between the pieces. Alternatively, some church floors featured a single layer of coarser mortar, with simpler tile shapes and larger joints. It is important to mention that interior church floors can undergo alterations over time, potentially involving the replacement of original mortars, or the introduction of newer materials, or even the placement of new coatings over the more primitive ones, which is why this type of coating was discovered at lower levels than the current floor (Rodwell, 2001).

The primitive ceramic floor pieces from the church of the monastery of Alcobaça exhibit the characteristic thickness and lateral chamfered edges of medieval pieces. However, specific information regarding the ground preparation layers, mortar characteristics, and installation methods is currently lacking. Studies of historic mortar flooring in a religious context are not common, owing to the challenge associated with uncovering them. Usually, publications of flooring studies concern the ceramic tiles themselves, without mentioning their fixing system or when specifically dedicated to mortars; the most frequent are in the context of mosaic floors (Fawcett, 2001; Norton, 1981; Orgeur, 2005; Rouzeau et al., 2013; Secco et al., 2018). It is also important to note that the history of alterations and abandonment of monasteries, especially after the extinction of religious orders (in 1834), can result in the loss of original materials considered simpler, such as ceramic pieces of the flooring and its mortars (Fawcett, 2001). Moreover, burials were common in church interiors, which meant that the floor had to be altered regularly. This question does not arise in Alcobaça, since the church was the royal pantheon for centuries, using funerary tombs, so there is no evidence of alterations to the floor for this purpose. Therefore, this study offers a unique opportunity to investigate a possible original mortar used in a medieval church floor, with the aim of finding its key characteristics and relating them to its specific function, in fixing the ceramic pavement, and to aspects related to the raw materials and their use.

METHODOLOGY

For this study, 21 samples of mortar still adhering to the 19 different ceramic pieces (Figure 1) were collected, both at the back of the pieces and on the sides. In two cases, mortar samples were also taken from the main face to assess their similarity to those on the opposite side, in contact with the ground.

The characterization of the samples was carried out using a set of analytical techniques designed to minimize sample consumption while maximizing retrieved information (Arizzi & Cultrone, 2021; Artioli, 2010; Balksten, 2010; Hughes & Callebaut, 2000; La Russa & Ruffolo, 2021). The methodology adopted allows us to obtain information both on the overall composition of the samples, including binder and aggregates, and focused chemical analysis, aimed at specific characteristics of these same components. The samples underwent two distinct preparation methods, tailored to the technical requirements of each analytical tool. A small portion was manually ground in an agate mortar, and a fragment representing an aggregated portion of the sample was mounted in epoxy resin and polished for point analyses in cross-section.

All samples were observed using two optical microscopes: a Leica S9I Greenough Stereozoom microscope equipped with a Leica apochromatic objective, with a focal length of

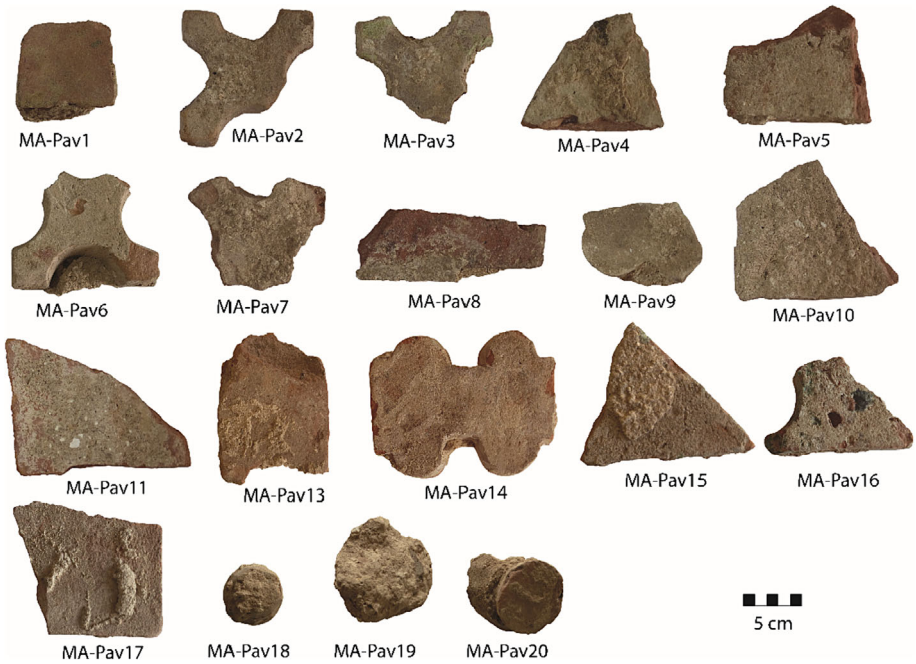

FIGURE 1 Single ceramic pieces that made up the early medieval pavement of the church of the Santa Maria de Alcobaça monastery, with traces of the laying mortar adhering to the side and back of the pieces. All the samples studied were collected from pieces stored under the same conditions of conditioning, lighting, temperature, and humidity.

50 mm, diameter of 58 mm and magnification ranging from 1.0 to 5.5×, and a Leica DMI5000 M inverted optical microscope with motorized stage, in reflected light. The motorized stage, microscope, and digital camera were controlled by Leica Application Suite software, version 4.12.0. Polarized light mode with 5.0× and 10.0× objectives allowed for detailed examination of the samples. The study of aggregate grain morphology utilized Image J software to analyze multiple images captured by optical microscopy, always at the same magnification. The apparent grain contours and size determination by Feret diameter were considered.

The color parameters L^*, a^*, b^* were determined using a portable colorimeter (Lovibond TR500 spectrophotometer). Measurements were performed in reflectance with a 4 mm aperture diameter, using Illuminant D65, observer 10°, and data acquisition OnShade QC v.1.7.2.520 software.

X-ray fluorescence for chemical analysis was performed using an X-ray fluorescence spectrometer with a wavelength-d system (WDXRF; PANalytical Axios 4.0), with a rhodium X-ray tube, under conditions optimized for element quantification. The analyzing crystals LiF220, LiF200, Ge, PE, and PX1 were used for the separation of fluorescent X-ray peaks covering the whole measurable range. Analysis was performed under He flow and spectral deconvolution was carried out using the iterative least-squares method and standardless semiquantitative analysis based on the fundamental parameter approach with the SuperQ IQ Plus software package (PANalytical BV, Almelo, Netherlands).

X-ray diffraction (XRD) analysis for the identification of mineralogical phases of the samples was performed using a PANalytical Xpert PRO MRD diffractometer, with an X'Celerator 1D detector and Cu Kα radiation at 45 kV and 40 mA settings, in the 2θ range of 10–65°, with steps of 0.02° and an acquisition time of 33 s per step, in continuous scan mode. The identification of crystalline phases was carried out using the X'Pert High Score Plus software.

Raman measurements were used for the identification of the aggregates and binder grain. The analyses were performed with a Renishaw inVia Qontor micro-Raman spectrometer equipped with an air-cooled CCD detector and an HeNe laser operating at 32 mW of 633 and 532 nm laser excitation. The spectral resolution of the spectroscopic system was 0.3 cm^{-1}. The laser beam was focused with a 50× or 100× Olympus objective lens (N10.6 LMPLAN FL N). All the raw data were collected digitally with Wire 5.1 software for processing. The minerals were identified using the Spectral ID database, version 9.2, part of the GRAMS Spectroscopy Software Suite, the RRUFF online database, and by comparing the results with the literature.

Thermo-analytical techniques—simultaneous differential thermal analysis (DTA) and thermogravimetry (TG)—were also used, using a SETARAM TG DTA 92-16.18 apparatus, incorporating a microbalance with a controlled argon gas flow (inert atmosphere). The samples were dried in an oven at 110°C for 2 h. Approximately 65 mg of milled sample was deposited in an alumina (α-Al_2O_3) crucible. The reference material was alumina powder, and the heating temperature range was from ambient to 1100°C, at a heating rate of 10°C min^{-1}.

Scanning electron microscopy (SEM) observation was performed on a Hitachi TM3030 Plus tabletop microscope, coupled with a Quantax70 energy-d X-ray spectrometer, operated at an acceleration voltage of 15 kV at ambient temperature and under low vacuum, without the need for prior sample preparation. Images were acquired in standard/charge-up reduction MIX mode (SE/BSE) at magnifications of 120 and 250×.

RESULTS

The chemical composition quantification of the samples was determined by WDXRF analysis. The results obtained show that all samples have the same main elements, with SiO_2 ranging from 14% to 69%, CaO ranging from 13% to 78%, and Al_2O_3 ranging from 3% to 10%. However, these extreme values do not reflect the majority of cases, as can be seen in Figure 2. On average, the compositions suggest a predominance of SiO_2 content in most instances. When considering the location of the mortar in the piece, it is also possible to observe that samples collected from the side (L) exhibit greater variation in the percentages of the main components compared to those collected from the back (T) of the pieces, which show more consistent CaO and SiO_2 contents. Regarding the other quantified elements, all samples showed similar percentages of Fe_2O_3, MgO, K_2O, and SO_3. Additionally, all samples contain trace percentages of PbO, typically below 1%, except for sample MA-Pav20, which exhibited a percentage of 5%. The high content of lead is attributed to the presence of small fragments of glaze that could remain attached to the mortar.

Table 1 presents the main mineral phases identified through XRD analysis. Quartz and calcite are consistently present in all samples, exhibiting the highest intensities. Notably, most samples, particularly those taken from the back of the pieces, display a predominant intensity of quartz peaks. In addition to these minerals, kaolinite and potassic feldspars such as microcline were also frequently identified, albeit with relatively low-intensity peaks. Other minerals were sporadically detected in specific samples, namely anorthite, muscovite, and hematite, always with low- to very low-intensity peaks. Despite variations in peak intensity, the crystalline phases identified by XRD were consistently present across all results, which may indicate a degree of uniformity in the raw material used for the preparation of the mortars.

Using SEM–energy-dispersive X-ray spectroscopy (EDS) and Raman spectroscopy it was possible to identify the distribution of these crystalline phases throughout the samples. SEM imaging with EDS mappings (Figure 3a) allowed the identification of O, C, and Ca concentrations in the zones of the samples corresponding to the binder. Concerning the aggregates, there is a predominance of grains composed of Si and O. Additionally, in all observed samples, grains

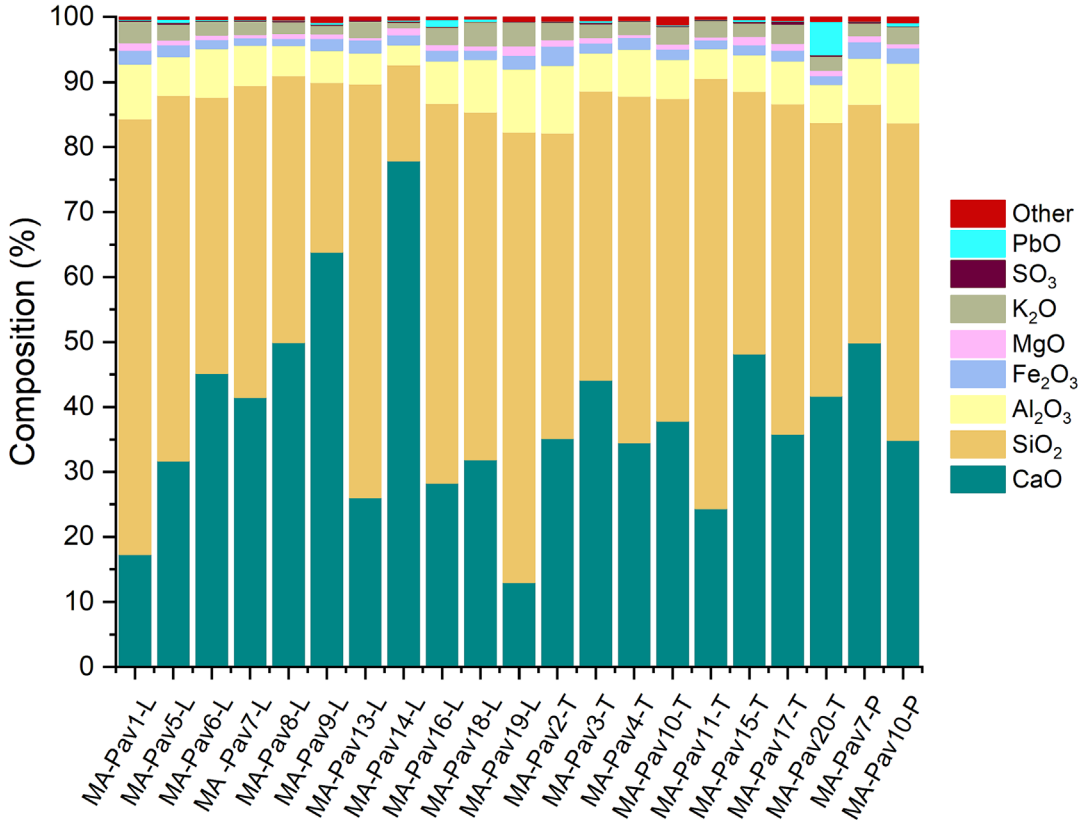

FIGURE 2 Overall chemical composition of the samples obtained by wavelength-dispersive X-ray fluorescence. In the sample name the final letter indicates the sampling location on the piece, where L = side, T = back and P = main face.

with a predominant composition in K, Al, O, and Si were identified, although these occurred less frequently compared to Si–O grains. In some samples, aggregates with elemental concentrations of Na, Al, O, and Si were also detected. This can be associated with the chemical composition of sodium feldspar (Na ($AlSi_3O_8$)), which was less frequently observed in the other samples. These findings align with the mineral phases identified by XRD. The most frequent composition mapped in all results corresponds to the chemical formula of quartz (SiO_2), mostly distributed by the mortar as the main mineral component of sands. Additionally, feldspar grains, mainly potassic ($K(AlSi_3O_8)$) and possibly sodic, were identified as the primary minerals associated with the aggregates of these mortars. Sporadically, it was also possible to observe the concentration of other elements quantified in lower percentages, such as Fe (on average, 1.72%), or very low as Mn (on average, 0.08%), in grains with elemental composition consistent with aluminosilicates.

μ-Raman spectroscopy confirmed the main minerals associated with both the binder and the aggregates. Figure 3b shows the characteristic bands of each of the identified minerals. Calcite was identified as the main mineral present in the zone corresponding to the binder in all samples. Regarding the aggregates, quartz was confirmed as the main and most abundant component in all samples (Kramar et al., 2010; Socrates, 2001). In some cases, it was also associated with other minerals, especially carbonaceous materials, where it was possible to observe the characteristic bands of the two components. Isolated grains of carbonaceous matter (Jehlička et al., 2017), possibly coal, were identified in some samples, as exemplified in the spectrum in

TABLE 1 Main crystalline phases identified by X-ray diffraction for the mortar samples of the primitive ceramic pavement of the church of the monastery of Alcobaça: quartz (Qz)—SiO_2; calcite (Cal)—$CaCO_3$; kaolinite (Kln)—$Al_2(Si2O_5)(OH)_4$; anorthite (An)—Ca ($Al_2Si_2O_8$), microcline (Mcc)—$K(AlSi_3O_8)$; muscovite (Ms)—$KAl_2(AlSi_3O_{10})(OH)_2$; hematite (Hem)—α-$Fe_2O_3$ (Warr, 2021).

Sample	Qz	Cal	Kln	An	Mcc	Ms	Hem
MA-Pav1-L	++++	++	+		+		
MA-Pav2-T	+++	++++	+		+		
MA-Pav3-T	++++	+++	+		++		
MA-Pav4-T	++++	++	+		+		
MA-Pav5-L	++++	++	+		+		
MA-Pav6-L	++++	++++	++		++		+
MA-Pav7-P	++++	++++	+		+		
MA-Pav7-L	++++	+++	+		+	+	
MA-Pav8-L	++++	+++			+		
MA-Pav9-L	+++	++++	+		+		
MA-Pav10-P	++++	+++	+		+	+	
MA-Pav10-T	++++	+++			++		
MA-Pav11-T	++++	+++			++		
MA-Pav13-L	++	++++					+
MA-Pav14-L	++++	+++	+	+	++		
MA-Pav15-T	++++	+++	+	+	++		
MA-Pav16-L	++++	+++	+		++		
MA-Pav17-T	++++	+++	+		++		
MA-Pav18-L	++++	++	+		++		
MA-Pav19-L	++++	+++	+	+	+		
MA-Pav20-T	++++	++	+	++			

Note: Relative intensity of diagnosis peaks: ++++ very intense; +++ intense; ++ weak; + very weak.

Figure 3b. In addition to these minerals, it was also possible to confirm the presence of grains of potassium feldspar (Freeman et al., 2008) as a constituent part of the aggregates in all samples. Other minerals were identified sporadically and in a smaller number of samples, such as goethite (α-$Fe^{3+}O(OH)$; de Faria & Lopes, 2007; RRUFF, no date-a). Among the less frequently identified minerals or components in the results, we highlight the identification of manganese oxide associated with some grains of the aggregates, in at least two of the samples. μ-Raman analysis was performed on the same grain shown in Figure 3a, on the Mn-rich grain boundary. The broad and intense band centered at 634 cm^{-1} is consistent with the results obtained by SEM-EDS and also with those presented in the literature (Bernardini et al., 2019). Another less frequently identified mineral was rutile (TiO_2), often associated with minerals of the kaolinite group (Wang et al., 2015), with the broadest band centered at 614 cm^{-1} attributed to rutile (RRUFF database). The other bands between 129 and 1049 cm^{-1}, indicated in the spectrum of Figure 3b, were attributed to the Al–O and Si–O vibrations of minerals of the kaolinite group (Kloprogge, 2017; Wang et al., 2015).

The floor mortars of the church of Santa Maria de Alcobaça are thus mainly composed of siliceous sand, with quartz being the most abundant mineral. Upon stereo microscopy observation of the samples, as collected, it is evident that lime lumps, traces of glaze, and even remnants of the ceramic body of the pieces are present in some cases, still adhering to the mortar. In general, the samples show good cohesion between the binder and the aggregate. In disaggregate

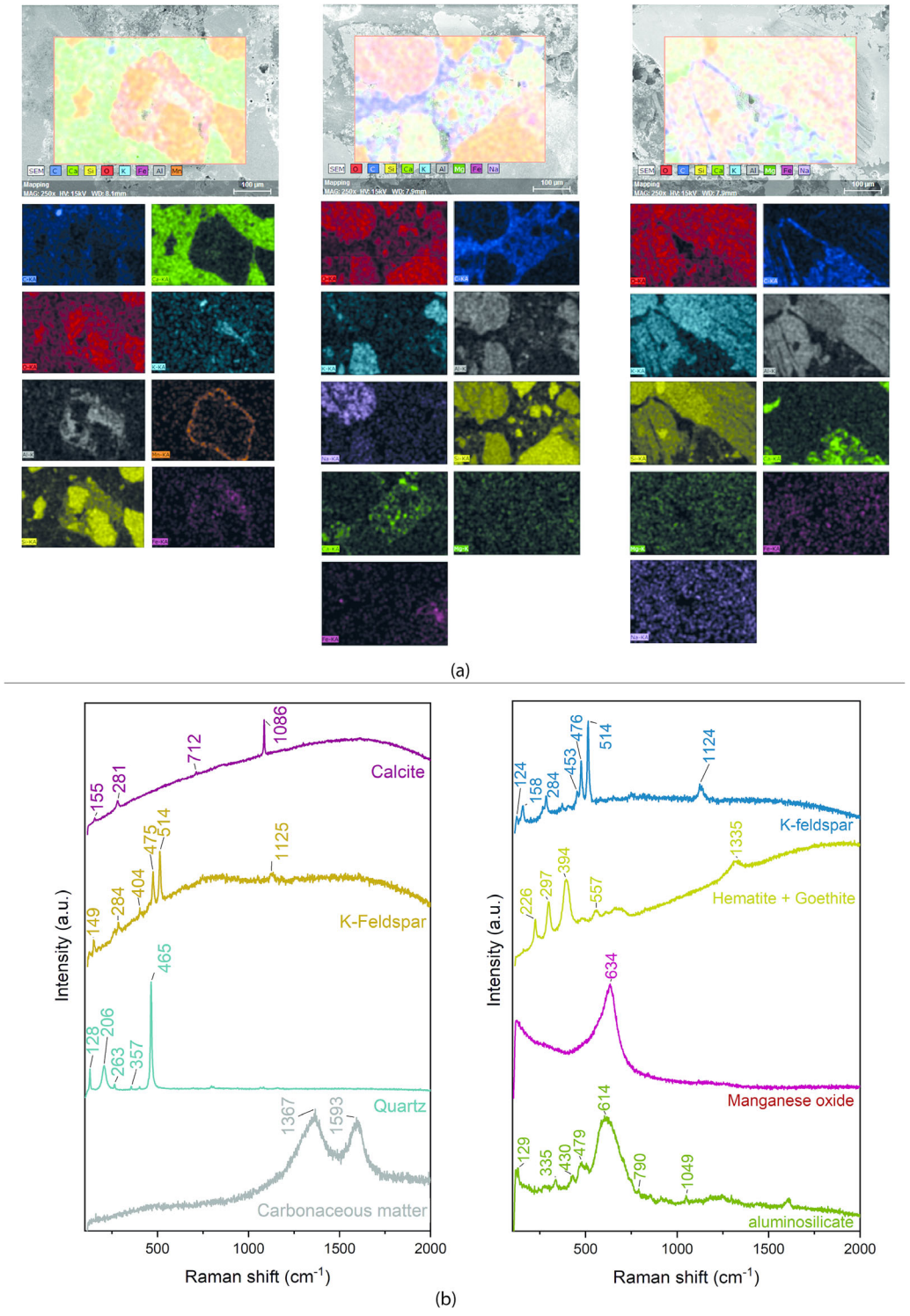

FIGURE 3 (a) Scanning electron microscopic images with energy-dispersive X-ray spectroscopic mappings to identify the specific composition of the aggregates. The elements K, Al, Si and O predominate in the zone corresponding to the aggregate, and Ca, C and O predominate in the zone corresponding to the binder. (b) Main results obtained by μ-Raman spectroscopy.

parts of the samples it was possible to observe that the sand particles are well graded, composed of grains ranging from angular, sub-angular and sub-rounded. In cross-section observation, sub-angular grains predominate. In cross-section optical microscopy, the distribution of aggregates within the binder is uniform, with some cases displaying a homogeneous distribution. Concerning the color parameters following the CIELab system, all samples display similar values for a^* and b^*, while the L^* parameter (representing lightness) displays the most significant variation, resulting in shades ranging from light beige to darker browns. The colorimetry measurements and their primary characteristics are detailed in Table 2. It is possible to observe that, in general, samples taken from the sides of the tiles exhibit lighter tones compared to samples collected from the back, although this pattern is not consistent across all cases. Regarding the size of the grains by the binder, it is possible to confirm the use of a well-graded sand, composed mostly of medium/coarse grains.

TG-DTA analysis was performed on a smaller subset of samples to assess mass losses during thermal analysis. Up to 600°C the mass losses are associated with the different types of water that the sample may contain: loss of moisture water, considered up to 120°C, is the first stage, followed by losses associated with water from hydrated compounds up to 200°C; finally, the loss of structural water of the compounds is considered up to 600°C. To understand the hydraulic properties of the mortars, the ratio between the loss of structural water and the loss of CO_2 was calculated. This ratio is inversely proportional to the loss of CO_2, meaning that lower CO_2 loss indicates greater hydraulic properties in the mortar (Biscontin et al., 2002; Elsen et al., 2013; Moropoulou et al., 2000; Pires & Cruz, 2007). The results reveal that the analyzed

TABLE 2 Colors of mortar samples, measured by colorimetry. Variation of the grain size of the aggregates and their distribution over the binder, observed in the samples in cross-section.

Sample	Color	L^*, a^*, b^*	Size variation (μm)	Average size (μm)	Aggregate abundance	Distribution
MA-Pav1-L		65.80, 5.55, 15.10	64.25–598.87	283.58	++++	Homogeneous
MA-Pav2-T		53.36, 6.89, 16.01	44.96–1538.91	254.97	+++	Heterogeneous
MA-Pav3-T		56.33, 5.63, 16.13	150.05–716.18	248.08	+++	Heterogeneous
MA-Pav4-T		51.25, 6.51, 16.91	97.39–790.75	393.13	+++	Heterogeneous
MA-Pav5-L		77.19, 3.81, 11.94	90.50–529.76	280.96	++++	Homogeneous
MA-Pav6-L		57.98, 5.72, 16.34	54.98–878.40	297.20	+++	Heterogeneous
MA-Pav7-L		45.36, 7.05, 14.02	69.32–760.72	273.61	+++	Homogeneous
MA-Pav8-L		56.02, 5.12, 14.23	112.86–840.34	367.21	+++	Heterogeneous
MA-Pav9-L		56.98, 5.59, 15.39	136.47–716.18	323.37	++++	Heterogeneous
MA-Pav10-P		46.81, 5.38, 15.08	172.74–575.18	336.00	++++	Heterogeneous
MA-Pav10-T		41.68, 5.28, 13.92	50.60–456.82	190.29	++++	Heterogeneous
MA-Pav11-T		42.81, 5.29, 9.96	66.02–985.93	328.97	+++	Heterogeneous
MA-Pav13-L		56.97, 5.78, 17.59	64.47–897.63	262.91	++	Heterogeneous
MA-Pav14-L		46.36, 6.55, 13.75	57.87–949.92	211.03	++++	Homogeneous
MA-Pav15-T		53.28, 7.14, 17.30	84.41–804.91	328.70	++++	Homogeneous
MA-Pav16-L		46.13, 5.44, 13.00	67.72–607.58	223.10	++++	Homogeneous
MA-Pav17-T		57.18, 4.56, 17.94	82.79–632.06	286.02	+++	Homogeneous
MA-Pav18-L		60.36, 5.39, 15.45	48.73–455.04	177.48	++++	Homogeneous
MA-Pav19-L		72.19, 4.20,13.52	74.54–1338.77	259.19	+++	Heterogeneous
MA-Pav20-T		52.69, 6.96, 16.45	98.29–520.90	232.73	++++	Heterogeneous

Note: Aggregate abundance: very abundant (++++), abundant (+++), less abundant (++).

TABLE 3 Results obtained by thermogravimetry–differential thermal analysis for water and CO_2 loss from some of the Alcobaça pavement mortar samples. Hydraulicity index calculated from the CO_2/H_2O ratio.

	H_2O loss (%)			CO_2 loss (%)			
Sample	**<120°C**	**120–200°C**	**200–600°C**	**600–800°C**	**800–1100°C**	**Total loss (%)**	**CO_2/H_2O**
MA-Pav3-T	1.22	0.59	2.14	5.75	10.89	20.60	7.79
MA-Pav5-L	1.81	1.32	2.67	5.81	7.14	18.75	4.85
MA-Pav7-L	0.90	0.50	1.89	5.23	12.22	20.74	9.21
MA-Pav10-P	1.08	0.76	2.55	5.68	8.68	18.75	5.63
MA-Pav14-L	1.19	0.66	1.70	4.61	15.73	23.89	11.99

mortars present varying degrees of hydraulic character, with values ranging from 4.85 to 9.21. Notably, only one of the samples displayed a value consistent with an aerial mortar (MA-Pav14-L) (Ergenç et al., 2021), and there was no distinct characteristic pattern observed across all cases (see Table 3).

DISCUSSION

The results suggest that the medieval ceramic floor of the Alcobaça church was laid using lime mortars and aggregates primarily composed of siliceous sand, with some hydraulic properties. During medieval times, it was common practice to use locally available raw materials and labor force for manufacturing and laying ceramic pavements (Durbin, 2005). Furthermore, the involvement of the Cistercian order in overseeing the work of the monks indicates that the entire process of preparing the mortar and laying the pavement relied on regionally accessible materials. Geologically, the Alcobaça region is situated to the west of the Serra dos Candeeiros, characterized by limestone outcrops primarily from the Jurassic period (Goulão et al., 2011;Inácio, 2023; Silva et al., 2022). Considering the current territory of the municipality, the region is also composed of geological formations of different ages, serving as potential sources of geological material. According to (Goulão et al., 2011):

> … the best represented rocks date from the Middle and Upper Jurassic and correspond to highly pure limestones (Middle Jurassic) and sandstones, claystone and more or less marly limestones (Upper Jurassic). The Cretaceous formations are represented by more or less consolidated sandstones and claystone and also by limestones characterized by the presence of abundant fossil fauna. The Paleogene, Miocene and Pliocene formations are essentially represented by sandy deposits.
>
> (Goulão et al., 2011, p. 7)

The Alcobaça region is thus rich in rocks of excellent quality for the production of lime and also for other uses, including for ornamental purposes, which are still being exploited today (Inácio, 2023; Silva et al., 2022). According to the literature, although there is no known systematic study on the provenance of the rocks used in the construction of the Alcobaça monastery, the authors believe in the local exploitation of rocks from the Serra dos Candeeiros as a source of raw material, since "there are traces of very old explorations, … In them, the marks resulting from the artisanal method of cutting by sledgehammer and pickaxe that lasted since the times of the Roman Empire are perfectly distinguishable" (Goulão et al., 2011, p. 8).

Additionally, the mineralogical composition of clays in the Alcobaça region is abundant in minerals like quartz and kaolinite, along with feldspars, particularly potassium and iron oxides (Lisboa, 2014). The presence of clay minerals in the limestone exploitation zone as a source of raw material can give rise to lime with a hydraulic character (Arizzi & Cultrone, 2013; Elsen et al., 2013), which may explain the results obtained by TG-DTA. The mineral phases identified by XRD in the mortar samples of the primitive ceramic pavement are coherent with the local geology, reinforcing the use of local raw materials for the preparation of materials used in monastic constructions, in accordance with the tradition valued by the Cistercian Order. Furthermore, the choice of a predominantly siliceous and well-graded sand for the mortar aligns with its intended function. Siliceous sands are more chemically resistant and provide increased volumetric resistance to the mortar. The presence of more angular grains and a well-graded sand helps fill voids effectively, resulting in a smaller macropore system and better adhesion to the binder. These characteristics have a direct impact on the mortar's strength, making it a suitable material for laying tiles and other applications (Arizzi & Cultrone, 2013; Artioli et al., 2019; Durbin, 2005; Santos et al., 2018; Stefanidou & Papayianni, 2005).

The samples collected from the sides of the ceramic pieces exhibited greater compositional variation compared to those collected from the backs of the ceramic pieces. This difference could be related to increased exposure of the mortars on the sides to wear from use, cleaning, or other factors such as floods, which were frequent in the church of Alcobaça.

CONCLUSIONS

The results obtained in this study indicate that the mortars used in the laying of the ceramic floor in the church of Santa Maria de Alcobaça present similar characteristics, in terms of their chemical composition, mineralogical constitution, and aggregate morphology. The observed characteristic features, notably the use of siliceous sand, with predominantly sub-angular, well-graded grains, primarily comprising medium to coarse grains, point to the formulation of a cohesive and resilient mortar, ideally suited for the purpose of laying pavements. However, it was observed that the samples taken from the sides of the ceramic tiles showed greater variation in overall chemical composition than the samples taken from the back, although no pattern was identified for all cases. When considering the characteristics of the aggregates in cross-section, we realized that the side samples tended to be slightly finer grained and, in some cases, less abundant than those observed in the back samples. Although a consistent pattern was not identifiable across all samples, there is a noticeable trend that aligns with the functional purpose of the materials. As the pieces were chamfered to allow space for the mortar to fill the sides, it is reasonable that the finer grains would occupy the narrower spaces, especially those close to the edges. Moreover, the friction of use and cleaning processes could cause a loss of granular material, which could result in the lower abundance of aggregates observed in some samples on the sides.

Regarding the mineralogy identified, in addition to the predominance of quartz, other minerals identified in smaller proportions, such as kaolinite, potassium feldspars and iron oxides, are part of the composition of the clays, which are common and abundant in this part of Portugal. The use of clays in the preparation of mortars results in a material with some degree of hydraulicity, which also contributes to the mechanical resistance so necessary for the function of these mortars. These observations align remarkably well with the geological profile of the Alcobaça region, suggesting the use of locally sourced raw materials in the mortar preparation. Furthermore, the literature suggests that the Cistercian Order, under whose auspices the monastic complex was established, often selected monastery locations based on the availability of natural resources and raw materials to fulfil the construction and operational requirements of the monasteries. Although further studies are necessary to confirm the dating of the samples,

the results obtained, combined with the historical and geological context of the monument and the region, allow us to infer that the analyzed mortar samples are contemporaneous with the construction period of the Alcobaça Monastery, potentially constituting the original mortars employed in the floor installation.

DATA AVAILABILITY STATEMENT

Data sharing not applicable to this article as no datasets were generated or analysed during the current study.

ORCID

Fernanda Carvalho https://orcid.org/0000-0002-3627-5060
João Pedro Veiga https://orcid.org/0000-0001-5324-1586

REFERENCES

Antunes, J. F. D. (2013). *Mosteiro de Santa Maria de Alcobaça—Análise das intervenções efectuadas nos últimos 50 anos, diagnóstico das anomalias actuais e proposta de intervenção futura*. Instituto Superior de Engenharia de Lisboa. Available at: https://repositorio.ipl.pt/bitstream/10400.21/…/1/dissertação.pdf

Arizzi, A., & Cultrone, G. (2013). The influence of aggregate texture, morphology and grading on the carbonation of non-hydraulic (aerial) limebased mortars. *Quarterly Journal of Engineering Geology and Hydrogeology*, *46*(4), 507–520. https://doi.org/10.1144/qjegh2012-017

Arizzi, A., & Cultrone, G. (2021). Mortars and plasters—How to characterise hydraulic mortars. *Archaeological and Anthropological Sciences*, *13*(9), 144. https://doi.org/10.1007/s12520-021-01404-2

Artioli, G. (2010). *Scientific methods and cultural heritage*. Oxford University Press. https://doi.org/10.1093/acprof:oso/9780199548262.001.0001

Artioli, G., Secco, M., & Addis, A. (2019). The Vitruvian legacy: Mortars and binders before and after the Roman world. *European Mineralogical Union Notes in Mineralogy*, *20*, 151–202. https://doi.org/10.1180/EMU-notes.20.4

Balksten, K. (2010). Understanding Historic Mortars and their Variations – a Condition for Performing Restorations with Traditional Materials. In *2nd conference on historic mortars—HMC 2010 and RILEM TC 203-RHM final workshop*, (September) (pp. 11–18).

Bernardini, S., Bellatreccia, F., Casanova Municchia, A., Della Ventura, G., & Sodo, A. (2019). Raman spectra of natural manganese oxides. *Journal of Raman Spectroscopy*, *50*(6), 873–888. https://doi.org/10.1002/jrs.5583

Biscontin, G., Pellizon Birelli, M., & Zendri, E. (2002). Characterization of binders employed in the manufacture of Venetian historical mortars. *Journal of Cultural Heritage*, *3*(1), 31–37. https://doi.org/10.1016/S1296-2074(02)01156-1

Carvalho, F., Coentro, S., Costeira, I., Trindade, R. A. A., Alves, L. C., da Silva, R. C., & Muralha, V. S. F. (2016). The Cistercian glazed tiles of the monastery of Alcobaça: Characterization of the colour palette. *Journal of Medieval Iberian Studies*, *8*(2), 196–216. https://doi.org/10.1080/17546559.2016.1222447

Colaço, J. (1932). Um Curioso Pavimento de Cerâmica no Mosteiro de Alcobaça. *Diário de Notícias*. 16 October

de Faria, D. L. A., & Lopes, F. N. (2007). Heated goethite and natural hematite: Can Raman spectroscopy be used to differentiate them? *Vibrational Spectroscopy*, *45*(2), 117–121. https://doi.org/10.1016/j.vibspec.2007.07.003

de Matos, C. A. (2019). *Os Boletins da Direcção-Geral dos Edifícios e Monumentos Nacionais*. Universidade do Porto.

Villamariz, C., & Madureira, A. (2012). *A Arquitectura Religiosa Gótica em Portugal no Século XIV: O tempo dos Experimentalismos*, PhD Proposal. Universidade Nova de Lisboa. https://doi.org/10.1017/CBO9781107415324.004

Durbin, L. (2005). *Architectural tiles: Conservation and restoration*. Elsevier.

Elsen, J., Van Balen, K., & Mertens, G. (2013). Hydraulicity in historic lime mortars: A review. In J. Válek, J. J. Hughes, & C. J. W. P. Groot (Eds.), *Historic mortars—Characterisation, assessment and repair. Rilem book* (pp. 121–136). Springer. https://doi.org/10.1007/978-94-007-4635-0

Ergenç, D., Fort, R., Varas−Muriel, M. J., & Alvarez de Buergo, M. (2021). Mortars and plasters—How to characterize aerial mortars and plasters. *Archaeological and Anthropological Sciences*, *13*(11), 197. https://doi.org/10.1007/s12520-021-01398-x

Fawcett, J. (2001). In J. Fawcett (Ed.), *Historic floors. Their care and consevation, Butterworth-Heinemann series in conservation and museology series*. Butterworth-Heinemann.

Ferreira, M. A. L. P. D. T. (1987). *Mosteiro de Santa Maria de Alcobaça–Roteiro* (2nd ed.). ELO.

Freeman, J. J., Wang, A., Kuebler, K. E., Jolliff, B. L., & Haskin, L. A. (2008). Characterization of natural feldspars by Raman spectroscopy for future planetary exploration. *Canadian Mineralogist*, *46*(6), 1477–1500. https://doi.org/10.3749/canmin.46.6.1477

Goulão, M., Rebelo, D., & Gomes, C. (2011). *PDM de Alcobaça*. A Pedra. March

Hughes, J. J., & Callebaut, K. (2000). Practical Sampling of Historic Mortars. In P. J. M. Bartos, C. Groot, & J. J. Hughes (Eds.), *International RILEM workshop on historic mortars: Characteristics and tests* (pp. 17–26). RILEM Publications SARL.

Inácio, T. (2023). Os Fornos Artesanais de Cal de Pataias (Alcobaça): Resultados preliminares do seu estudo. *Estudos Arqueológicos de Oeiras*, *32*, 379–404. https://doi.org/10.5281/zenodo.7920571

Jehlička, J., Culka, A., & Košek, F. (2017). Obtaining Raman spectra of minerals and carbonaceous matter using a portable sequentially shifted excitation Raman spectrometer—A few examples. *Journal of Raman Spectroscopy*, *48*(11), 1583–1589. https://doi.org/10.1002/jrs.5105

Kloprogge, J. T. (2017). Raman spectroscopy of clay minerals. In *Developments in clay science* (1st ed.) (pp. 150–199). Elsevier Ltd.. https://doi.org/10.1016/B978-0-08-100355-8.00006-0

Kramar, S., Urosevic, M., Pristacz, H., & Mirtič, B. (2010). Assessment of limestone deterioration due to salt formation by micro-Raman spectroscopy: Application to architectural heritage. *Journal of Raman Spectroscopy*, *41*(11), 1441–1448. https://doi.org/10.1002/jrs.2700

La Russa, M. F., & Ruffolo, S. A. (2021). Mortars and plasters—How to characterize mortar and plaster degradation. *Archaeological and Anthropological Sciences*, *13*(10), 165. https://doi.org/10.1007/s12520-021-01405-1

Lisboa, J. V. V. (2014). *Argilas comuns em Portugal Continental: Ocorrência e caraterísticas* (pp. 136–164). Associação Portuguesa para o Estudo do Quaternário (APEQ).

Martins, A. M. T. (2011). Património arquitectónico cisterciense : Um contínuo testemunho. In *Simpósio Património Em Construção: Contextos Para a Sua preservação* (pp. 25–32). Available at: https://ubibliorum.ubi.pt/bitstream/10400.6/691/1/A_MARTINS_LNEC.pdf

Martins, P. M. G. (2015) *A evolução morfológica e funcional dos Coutos do Mosteiro de Alcobaça – Uma experiência de Ensino*.

Moropoulou, A., Bakolas, A., & Bisbikou, K. (2000). Investigation of the technology of historic mortars. *Journal of Cultural Heritage*, *1*(1), 45–58. https://doi.org/10.1016/S1296-2074(99)00118-1

Norton, C. (1981). Les carreaux de pavage du Moyen Age de l'abbaye de Saint-Denis. *Bulletin Monumental*, *139*(2), 69–100. https://doi.org/10.3406/bulmo.1981.5977

Orgeur, M. (2005). Les carreaux de pavement des abbayes cisterciennes en Bourgogne (Fin XIIe -Fin XIVe siècle). *Bulletin du Centre d'études médiévales d'Auxerre|BUCEMA*, *9*(2006), 1–7. https://doi.org/10.4000/cem.850

Pires, J., & Cruz, A. J. (2007). Techniques of thermal analysis applied to the study of cultural heritage. *Journal of Thermal Analysis and Calorimetry*, *87*(2), 411–415. https://doi.org/10.1007/s10973-004-6775-0

Rodwell, W. (2001). The archaeology of church and cathedral floors. In J. Fawcett (Ed.), *Historic floors: Their care and conservation* (pp. 41–52). Butterworth-Heinemann.

Rouzeau, B., Bocquet-Lienard, A., & Moulis, C. (2013). Les carreaux de pavement découverts à l'abbaye de Morimond (Haute-Marne) : étude typologique, technique et archéométrique. *Revue archéologique de l'Est*, *6273*(Tome 62), 343–366.

RRUFF. (no date-a) *Goethite X050091*. Available at: https://rruff.info/goethite/display=default/X050091 (Accessed: 5 December 2022).

RRUFF. (no date-b) *Rutile R050031*. Available at: https://rruff.info/rutile/display=default/R050031 (Accessed: 2 December 2022).

Santos, A. R., Veiga, M. R., Santos Silva, A., de Brito, J., & Álvarez, J. I. (2018). Evolution of the microstructure of lime based mortars and influence on the mechanical behaviour: The role of the aggregates. *Construction and Building Materials*, *187*, 907–922. https://doi.org/10.1016/j.conbuildmat.2018.07.223

Secco, M., Dilaria, S., Addis, A., Bonetto, J., Artioli, G., & Salvadori, M. (2018). The evolution of the Vitruvian recipes over 500 years of floor-making techniques: The case studies of the Domus delle bestie Ferite and the Domus di Tito Macro (Aquileia, Italy). *Archaeometry*, *60*(2), 185–206. https://doi.org/10.1111/arcm.12305

Silva, T. P., de Oliveira, D., Veiga, J. P., Lisboa, V., Carvalho, J., Barreiros, M. A., Coutinho, M. L., Salas-Colera, E., & Vigário, R. (2022). Contribution to the understanding of the colour change in bluish-grey limestones. *Heritage*, *5*(3), 1479–1503. https://doi.org/10.3390/heritage5030078

Simões, S. (1990). *A Azulejaria em Portugal nos Séculos XV e XVI* (2a ed.). Fundação Calouste Gulbenkian.

Socrates, G. (2001). Infrared and Raman characteristic group frequencies. Tables and charts. *Journal of Raman Spectroscopy*. Available at:. https://doi.org/10.1002/jrs.1238

Stefanidou, M., & Papayianni, I. (2005). The role of aggregates on the structure and properties of lime mortars. *Cement and Concrete Composites*, *27*(9–10), 914–919. https://doi.org/10.1016/j.cemconcomp.2005.05.001

Trindade, R. A. A. (1998). Identificação de Azulejos Figurativos em Técnica de Linha Incisa na Abadia de Santa Maria de Alcobaça. *Olaria: Estudos Arqueológicos, Históricos e Etinológicos*, *2*, 144–148.

Trindade, R. A. A. (2007). In F. M. de Ferro (Ed.), *Revestimentos Cerâmicos Portugueses—Meados do século XIV à primeira metade do século XVI* (Edições Co, Edições Colibri. Edições Co ed.). Faculdade de Ciências Sociais e Humanas da Universidade Nova de Lisboa.

Trindade, R. A. A. (2018). Ceramic flooring from the Cistercian Abbey of Santa Maria de Alcobaça, Portugal (13th and 14th centuries). *Medieval Ceramics*, *37*, 79–85.

Wang, A., Freeman, J. J., & Jolliff, B. L. (2015). Understanding the Raman spectral features of phyllosilicates. *Journal of Raman Spectroscopy*, *46*(10), 829–845. https://doi.org/10.1002/jrs.4680

Warr, L. N. (2021). IMA–CNMNC approved mineral symbols. *Mineralogical Magazine*, *85*(3), 291–320. https://doi.org/10.1180/mgm.2021.43

How to cite this article: Carvalho, F., Nunes, A., Pagará, A., Costeira, I., da Silva, T. P., Lima, M. M. R. A., & Veiga, J. P. (2024). Historical lime-based flooring mortars from the Church of Santa Maria de Alcobaça monastery (12th century), Portugal: A multi-analytical approach. *Archaeometry*, 1–14. https://doi.org/10.1111/arcm.12971